Fermi National Accelerator Laboratory

FERMILAB-Pub-94/012-E

E789

Nuclear Dependence of Neutral D-Meson Production by 800 GeV/c Protons

M.J. Leitch et al.
The E789 Collaboration

Fermi National Accelerator Laboratory
P.O. Box 500, Batavia, Illinois 60510

January 1994

Submitted to *Physical Review Letters*

Operated by Universities Research Association Inc. under Contract No. DE-AC02-76CHO3000 with the United States Department of Energy

Disclaimer

Nuclear Dependence of Neutral D-Meson Production by 800 GeV/c Protons

M. J. Leitch,[1] J. Boissevain,[1] T. A. Carey,[1] D. M. Jansen,[1]
R. G. Jeppesen,[1,*] J. S. Kapustinsky,[1] D. W. Lane,[1,†]
J. W. Lillberg,[1] P. L. McGaughey,[1] J. M. Moss,[1] J. C. Peng,[1]
L. D. Isenhower,[2] M. E. Sadler,[2] R. Schnathorst,[2,‡] G. Gidal,[3]
P. M. Ho,[3] M. S. Kowitt,[3,§] K. B. Luk,[3] D. Pripstein,[3]
L. M. Lederman,[4,||] M. H. Schub,[4] C. N. Brown,[5] W. E. Cooper,[5]
H. D. Glass,[5] K. N. Gounder,[5,¶] C. S. Mishra,[5] D. M. Kaplan,[6]
W. R. Luebke,[6] V. M. Martin,[6,**] R. S. Preston,[6] J. Sa,[6]
V. Tanikella,[6] R. Childers,[7] C. W. Darden,[7] J. R. Wilson,[7]
Y. C. Chen,[8,††] G. C. Kiang,[9] and P. K. Teng,[9]

[1] *Los Alamos National Laboratory, Los Alamos, New Mexico 87545*
[2] *Abilene Christian University, Abilene, Texas 79699*
[3] *Lawrence Berkeley Laboratory and University of California, Berkeley, California 94720*
[4] *University of Chicago, Chicago, Illinois 60637*
[5] *Fermi National Accelerator Laboratory, Batavia, Illinois 60510*
[6] *Northern Illinois University, DeKalb, Illinois 60115*
[7] *University of South Carolina, Columbia, South Carolina 29208*
[8] *Institute of Physics, National Cheng Kung University, Tainan, Taiwan*
[9] *Institute of Physics, Academia Sinica, Taipei, Taiwan*

(Received February 8, 1994)

The nuclear dependence for 800 GeV/c proton production of neutral D mesons has been measured near $x_F = 0$ in Experiment 789 at Fermilab. D mesons from beryllium and gold targets were detected with a pair spectrometer and a silicon vertex detector via their decay $D \to K\pi$. No nuclear dependence is found, with a measured $\alpha = 1.02 \pm 0.03 \pm 0.02$, in contrast to the large suppression seen previously for production of J/ψ and ψ'. The measured differential cross section, $d\sigma/dx_F$, for neutral D-meson production at $< x_F >= 0.031$ is $58 \pm 3 \pm 7$ μb/nucleon. The integrated cross section obtained by extrapolation of the measured cross section to all x_F is $17.7 \pm 0.9 \pm 3.4$ μb/nucleon and is consistent with previous measurements.

PACS number: 25.40.Ve, 13.85.Ni, 24.85.+p

A strong suppression of J/ψ and Υ production has been observed in p-A collisions on heavy relative to light nuclear targets[1–4]. Similar effects have been seen in heavy-ion collisions[5]. The causes of this suppression are still unclear; for example, one of the models discussed involves the conversion of J/ψ's into open-charm pairs ($D\bar{D}$) through interaction with co-movers or with the nucleus[6]. For D meson production this mechanism would be absent. Other mechanisms, such as effects in the initial state or effects on the gluon structure function, might impact charmonium production and open-charm production in similar ways. These issues have been the subject of a vast amount of theoretical activity [6–11]. Data on the nuclear dependence of D-meson production can help to identify the dynamics involved in these suppressions. Previous measurements for proton production of D mesons are few and did not explicitly reconstruct the D[12, 13].

We report results for D-meson production from Fermilab Experiment 789, in which over 4000 $D^0 \rightarrow K\pi$ decays have been reconstructed from 800 GeV/c protons incident on beryllium and gold targets. Throughout the paper, except where explicit charged decay products are listed, we use D^0 to refer to both the D^0 and its anti-particle, the $\bar{D}^0$.

Experiment 789 used an upgraded version of the pair spectrometer in the Fermilab Meson East beamline, previously used for experiments 605[14] and 772[1]. Thin strip targets of beryllium and gold (either 160 $\mu\mathrm{m}$ high by 1.8 mm long or 110 $\mu\mathrm{m}$ high by 0.8 mm long) localized the primary interaction point to a small region and downstream decays of neutral D mesons were identified using a silicon vertex detector. The silicon vertex detector consisted of sixteen 50 $\mu\mathrm{m}$ pitch silicon strip detectors each 5 x 5 cm^2 in area and 300 $\mu\mathrm{m}$ thick, covering an angular range of 20 to 60 mr above and below the beam axis. The detectors were positioned between 37 and 94 cm downstream of the target and were oriented to measure either the y(vertical) or u/v coordinates ($\pm5^\circ$ stereo angles). A total of 8,544 strips were individually read out via Fermilab amplifier cards[15] and LBL discriminators[16]. A vertex processor[17] provided on-line rejection of prompt target dihadron events by selecting only track pairs consistent with decay vertices at least 1.02 mm downstream of the target and impact parameters of at least 51 $\mu\mathrm{m}$ relative to the target center. Rejection factors between 5 and 20 were achieved, depending on the luminosity.

For these data two magnetic-field settings of the first spectrometer magnet (SM12) were used, 1000 amperes (1000A) and 900 amperes (900A). The nuclear-dependence measurement is based only on the 900A runs, in which both beryllium and gold targets were used, while at 1000A substantial data were obtained only for the gold target. With beam rates between 0.5 and 1.9×10^9 protons/sec, and a typical targeting fraction of ~ 0.4, total per nucleon luminosities of $17\ \mathrm{pb}^{-1}$ (900A beryllium), $13\ \mathrm{pb}^{-1}$ (900A gold), and $35\ \mathrm{pb}^{-1}$ (1000A gold) were obtained. This resulted in average multiplicities on each silicon plane between 5 and 13 hits per event. Approximately 380 million events were recorded on tape.

Beam flux normalization was obtained from a four-element scintillator telescope viewing the target at 90°, which was calibrated for each target by scanning the target vertically across the full vertical extent of the beam. This determined the relationship between counts in the 90° monitor and in the secondary-emission monitor (SEM) which intercepted the entire proton beam. The 90° monitor was then used to measure the actual proton flux incident on the target at its normal vertical position. For the beryllium target a substantial target-out background was determined and corrected for. This contributed about 4% to the relative uncertainty between the beryllium and gold data. The SEM calibration, determined using activation techniques, was $1.0 \pm 0.1 \times 10^6$ protons per SEM count.

Mass spectra for the three target and magnetic-field combinations are shown in Fig. 1. Background dihadron events from the target are rejected by requiring that events have a proper-lifetime significance, τ/σ, greater than 7.2, where τ is the proper lifetime of the downstream decay and σ is the corresponding uncertainty (typically $\sim 0.08\mathrm{ps}$). Each plot contains two entries per event, one assuming $D^0 \rightarrow \pi^+ K^-$ and the other $\bar{D}^0 \rightarrow \pi^- K^+$. Since the correct decay-product assignment gives a sharp peak in mass with $\sigma \simeq 5\ \mathrm{MeV/c^2}$ while the incorrect assignment gives $\sigma \simeq 50\ \mathrm{MeV/c^2}$, only the correct assumption contributes to the clear peak at the D^0 mass of $1.86\ \mathrm{GeV/c^2}$. The continuum background underneath the peak is mostly from target hadron pairs misidentified as downstream events by the vertex detector. Since the rates in the silicon vertex detector are higher at 900A for gold than for beryllium, this continuum background is higher by approximately a factor of 1.6 for gold due to the increased tracking confusion in the silicon detector. To obtain the sum of the D^0 and $\bar{D}^0$ yields, the spectra were fit with a narrow gaussian and a wide gaussian, representing the correct particle and decay assumption and the incorrect assumption, respectively, with a polynomial background underneath these peaks. The wide peak was constrained to have the same number of counts as the narrow peak, since in this summed spectrum each D^0 or $\bar{D}^0$ event will give one entry in each peak. In order to determine the asymmetry between D^0 and $\bar{D}^0$ production another fit was done which allowed the D^0 and $\bar{D}^0$ to vary independently. A simultaneous fit to separate mass spectra for the two assumptions was done, similar to that described above, except that the narrow peak in each spectrum is constrained to the same area as the wide peak in the other spectrum.

The top panel in Fig. 1 shows the 900A beryllium mass spectrum for the loosest vertex cut. Several different lifetime-significance cuts have been studied to verify that no unexpected systematic effects from this cut occur. Detailed monte-carlo simulations of the system are used to determine the acceptance, including the effects of low-momentum pion tracks from the target in the silicon vertex detector, random hits in all the detectors, multiple scattering and decay of the produced particles, and efficiencies of all the detectors. The acceptances, including efficiencies, are about 1.4×10^{-3} (900A) and 6.4×10^{-4} (1000A). Additional vertex efficiences resulting from the lifetime significance cut of 7.2 used in Fig. 1 are about 0.19 (900A) and 0.24 (1000A). We use a D^0 lifetime of 0.420 ± 0.008 ps [18] and for the D^0 x_F and p_T distributions we use the average of the results obtained using the forms of Ref. [19] and Ref. [20]. The difference in acceptance obtained using these two parameterizations is about 10%. The efficiency of the level-one trigger was evaluated using prescaled minimum-bias triggers and was found to be 0.42 $\pm$ 0.04 (900A) and 0.46 $\pm$ 0.04 (1000A). The additional efficiency factor from the vertex processor was evaluated by studying level-one triggers which were forced to pass the processor and was found to vary between 0.70 and 0.74.

We have checked our data against the published D^0 lifetime by determining the normalized D^0 yields corrected for acceptance effects in five bins of proper lifetime. All three samples give lifetimes consistent with the value used above. A fit to our combined data sample, shown in Fig. 2, yields a lifetime of 0.413 ± 0.018 ps.

The nuclear-dependence ratio from the 900A data is

$$R = \frac{\sigma(Au)/197}{\sigma(Be)/9} = 1.06 \pm 0.11(stat.) \pm 0.07(syst.),$$

corresponding to $\alpha = 1.02 \pm 0.03 \pm 0.02$, where α is the parameter obtained by representing the dependence of the cross section on atomic mass (A) as $\sigma(A) = \sigma_0 A^\alpha$. The uncertainty in the ratio is dominated by fitting and statistics ($\pm 10\%$), processor efficiency ($\pm 4\%$), and the relative luminosity ($\pm 4\%$). No asymmetry between D^0 and $\bar{D}^0$ production is seen, with $\sigma(D^0)/\sigma(\bar{D}^0) = 0.97 \pm 0.12$. Our data cover the ranges $0.0 < x_F < 0.08$ with $< x_F >= 0.031$ and $0.0 < p_T < 1.1$ GeV/c with $< p_T >= 0.50$ GeV/c. Using a $D^0 \to K\pi$ branching ratio of 0.0365 ± 0.0021[18] and assuming no nuclear dependence, we obtain a differential cross section for neutral D-meson production of $d\sigma/dx_F(D^0) + d\sigma/dx_F(\bar{D}^0) = 58 \pm 3 \pm 7$ μb/nucleon per unit x_F. The main uncertainties in this result include the proton beam flux ($\pm 10\%$), the $D^0 \to K\pi$ branching ratio ($\pm 5.8\%$), fitting and statistics ($\pm 4.9\%$), the trigger efficiency ($\pm 3.2\%$), the D^0 lifetime ($\pm 3\%$), and the processor efficiency ($\pm 2\%$). Using the average acceptance obtained from the p_T and x_F parameterizations of Refs. [19] and [20] to integrate over all x_F and p_T, we can also obtain the total cross section: $\sigma(D^0) + \sigma(\bar{D}^0) = 17.7 \pm 0.9 \pm 3.4$ μb/nucleon. This result includes an additional uncertainty of $\pm 15\%$, corresponding to the difference between the two parameterizations and their uncertainties. We have also studied the variation in α over our range in x_F and p_T. The results, shown in Table 1, exhibit no dependence on p_T and a slight but statistically insignificant decrease between the smaller and larger bin in x_F. Finally, our measured $d\sigma/dp_T$ for our best statistics data set, the one at 1000A, is shown in Fig. 3. A fit to the standard form $d\sigma/dp_T \propto p_T e^{-np_T^2}$ gives $n = 0.91 \pm 0.12$ (GeV/c)$^{-2}$.

Previous measurements of α for D-meson production have yielded values between 0.75 and 1.04. Recent results from E769 for 250 GeV/c pions yielded $\alpha = 1.00 \pm 0.05 \pm 0.02$ [21], in agreement with our result. Other measurements for 340 GeV/c pions from WA82[22] at $< x_F > = 0.24$ gave 0.92 ± 0.06 for all D's and 1.03 ± 0.11 for $D^0 \to K\pi$, also roughly in agreement. Both of these measurements cover a much wider range in x_F than do ours. Older results from beam-dump measurements using prompt single muons[12] or prompt neutrinos[13] yielded values of α substantially below one. These measurements all have acceptance primarily in the large x_F region above $x_F = 0.5$. They are also more indirect measurements, since the D mesons are not explicitly reconstructed, and rely upon several large corrections. Finally, we recall the nuclear dependences of J/ψ and ψ' production from Refs. [1, 23], which show an increasing suppression for larger x_F. Several of the mechanisms which can produce large suppressions have strong dependences on x_F. At large enough x_F of a single detected D meson, the x_2 (momentum fraction of the target parton) corresponding to the $D\bar{D}$ pair can be very small and may be influenced by shadowing of the gluon structure function. Following Ref. [24], the strength of gluon shadowing must be less than that for sea quarks and could cause, at most, a reduction in α for the total D cross section to 0.96. However, the effect in a particular region in x_2 could be more dramatic. We have used the correlation measurements of E653[25] to estimate that the range of x_2 in our data lies above 0.05, well above the shadowing region. However, for the beam-dump measurements discussed above with $x_F \geq 0.5$, the $D\bar{D}$ x_2 would be substantially smaller, and shadowing may be causing all or part of the large suppression seen in these results.

Another model which predicts a strong suppression at large x_F, and could also explain the difference between the low- and high-x_F measurements of the nuclear dependence, is intrinsic charm[6]. This model gives an effect which depends strongly on x_F. Used within a two-component model which also includes the standard gluon-fusion picture modified by shadowing and various final-state effects, it appears to be able to explain the bulk of charm-production data. However, recent measurements by our group of J/ψ production at very large x_F[23] disagree with the shape of the x_F distribution predicted by this model.

Two previous measurements of the 800 GeV/c proton production cross section for neutral D mesons have been reported: E653 reported $38 \pm 3 \pm 13\ \mu\mathrm{b}$ [19], while E743 reported $22^{+9}_{-7} \pm 5.5\ \mu\mathrm{b}$ [20]. Our result is consistent with both but agrees best with that of E743.

In conclusion, the lack of nuclear dependence in the production of neutral D mesons suggests that the strong dependence seen in the production of J/ψ and ψ' is not the result of initial state effects or of nuclear modification of the gluon structure functions outside of the shadowing region. Other data on D-meson production that lie primarily in the large-x_F region, along with our results and those from several pion-beam experiments which lie primarily in the low-x_F region, suggest that shadowing or possibly intrinsic charm may play important roles in determining the nuclear dependences of open- and closed-charm production.

We wish to thank J. Appel, S. Brodsky, M. Strikman, and R. Vogt for useful discussions and also the Fermilab Research and Accelerator Divisions. This work was supported by the U. S. Department of Energy and the National Science Foundation.

REFERENCES

* Present Address: Science Applications International Corp., 2950 Patrick Henry drive, Santa Clara, CA 95054.

† Present Address: Department of Physics, Iowa State University, Ames, Iowa 50011.

‡ Present Address: Department of Physics, Purdue University, Lafayette, Indiana 47907.

§ Present Address: NASA/Goddard Space Flight Center, Greenbelt, Maryland 20771.

‖ Present Address: Department of Physics, Illinois Institute of Technology, Chicago, Illinois 60616.

¶ Present Address: Department of Physics, University of Mississippi, University, Mississippi 38677.

** Present Address: Department of Electrical Engineering and Computer Science, University of Illinois at Chicago, Chicago, Illinois 60680.

†† Also at Institute of Physics, Academia Sinica, Taipei, Taiwan.

[1] D. M. Alde *et al.*, Phys. Rev. Lett. **66**, 133 (1991); and Phys. Rev. Lett. **66**, 2285 (1991).

[2] S. Kartik *et al.*, Phys. Rev. D **41**, 1 (1990).

[3] S. Katsanevas *et al.*, Phys. Rev. Lett. **60**, 2121 (1988).

[4] J. Badier *et al.*, Z. Phys. C **20**, 101 (1983).

[5] C. Baglin *et al.*, Phys. Lett. **220**, 471 (1989); Phys. Lett B **255**, 459 (1991); and Phys. Lett B **270**, 105 (1991).

[6] R. Vogt, S. J. Brodsky, and P. Hoyer, Nucl. Phys. **B360** 67, (1991); **B383**, 643 (1992).

[7] Stanley J. Brodsky and Paul Hoyer, Phys. Rev. Lett. **63** 1566, (1989).

[8] S. Gavin and R. Vogt, Nucl. Phys. **B345** 104, (1990).

[9] S. Gavin and J. Milana, Brookhaven preprint BNL-46793.

[10] J.-P. Blaizot and J.-Y. Ollitrault, Phys. Lett. B **217**, 386 (1989).

[11] C. Gerschel and J. Hufner, Phys. Lett. B **207**, 253 (1988).

[12] H. Cobbaert *et al.*, Phys. Lett. **191**, 456 (1987) and **206**, 546 (1988).

[13] M. E. Duffy *et al.*, Phys. Rev. Lett. **55**, 1816 (1985).

[14] J. A. Crittenden *et al.*, Phys. Rev. D **34**, 2584 (1986); G. Moreno *et al.*, Phys. Rev. D **43**, 2815 (1991).

[15] D. Christian *et al.*, IEEE Trans. Nucl. Sci. **36**, 507 (1989).

[16] B. T. Turko *et al.*, IEEE Trans. Nucl. Sci. **39**, 758 (1992).

[17] C. Lee *et al.*, IEEE Trans. Nucl. Sci. **38**, 461 (1989).

[18] Particle Data Group: K. Hikasa *et al.*, Phys. Rev. D **45**, S1 (1992).

[19] K. Kodama *et al.*, Phys. Lett. **B263**, 573 (1991).

[20] R. Ammar *et al.*, Phys. Rev. Lett. **61**, 2185 (1988).

[21] G. A. Alves *et al.*, Phys. Rev. Lett. **70**, 722 (1993).

[22] M. Adamovich *et al.*, Phys. Lett. B **284**, 453 (1992).

[23] M. S. Kowitt, Ph. D. Thesis, U. of Calif. Berkeley, LBL-33331/UC-414 (1992); and M. S. Kowitt *et al.*, to be published.

[24] Jianwei Qiu, Phys. Lett. B **191**, 182 (1987).

[25] K. Kodama *et al.*, Phys. Lett. B **263**, 579 (1991).

FIGURES

FIG. 1. Invariant mass spectra for the three target and magnet-current configurations: 900 ampere SM12 magnet current (900A) for the beryllium (Be) and gold (Au) targets and 1000 ampere current (1000A) for the gold target. The peak at 1.86 GeV/c^2 corresponds to $D^0 \rightarrow K^- \pi^+$ and $\bar{D^0} \rightarrow K^+ \pi^-$ events. The bottom three panels are for the nominal lifetime significance cut ($\tau/\sigma > 7.2$). The top panel illustrates the degradation in peak to background ratio for the 900A Be data with a looser lifetime significance cut ($\tau/\sigma > 3.5$).

FIG. 2. Differential cross section per nucleon, $d\sigma/d\tau(D^0) + d\sigma/d\tau(\bar{D^0})$, versus proper lifetime (τ). Uncertainties shown are statistical only and do not include an additional systematic uncertainty of 12.8%. The solid line represents the fit used to obtain a $D^0 + \bar{D^0}$ lifetime of 0.413 ± 0.018 ps.

FIG. 3. Differential cross section per nucleon, $d\sigma/dp_T(D^0) + d\sigma/dp_T(\bar{D^0})$, versus p_T for our 1000A data. Uncertainties shown are statistical only and do not include an additional systematic uncertainty of 12.8%. The solid line represents the fit described in the text.

TABLES

TABLE I. Dependence of α for D^0 production on x_F and p_T. Uncertainties shown are statistical only and do not include an additional systematic uncertainty of 6%.

$< x_F >$	α	$< p_T >$ (GeV/c)	α
0.021	1.10 ± 0.04	0.31	1.05 ± 0.04
0.053	0.95 ± 0.05	0.75	1.05 ± 0.05

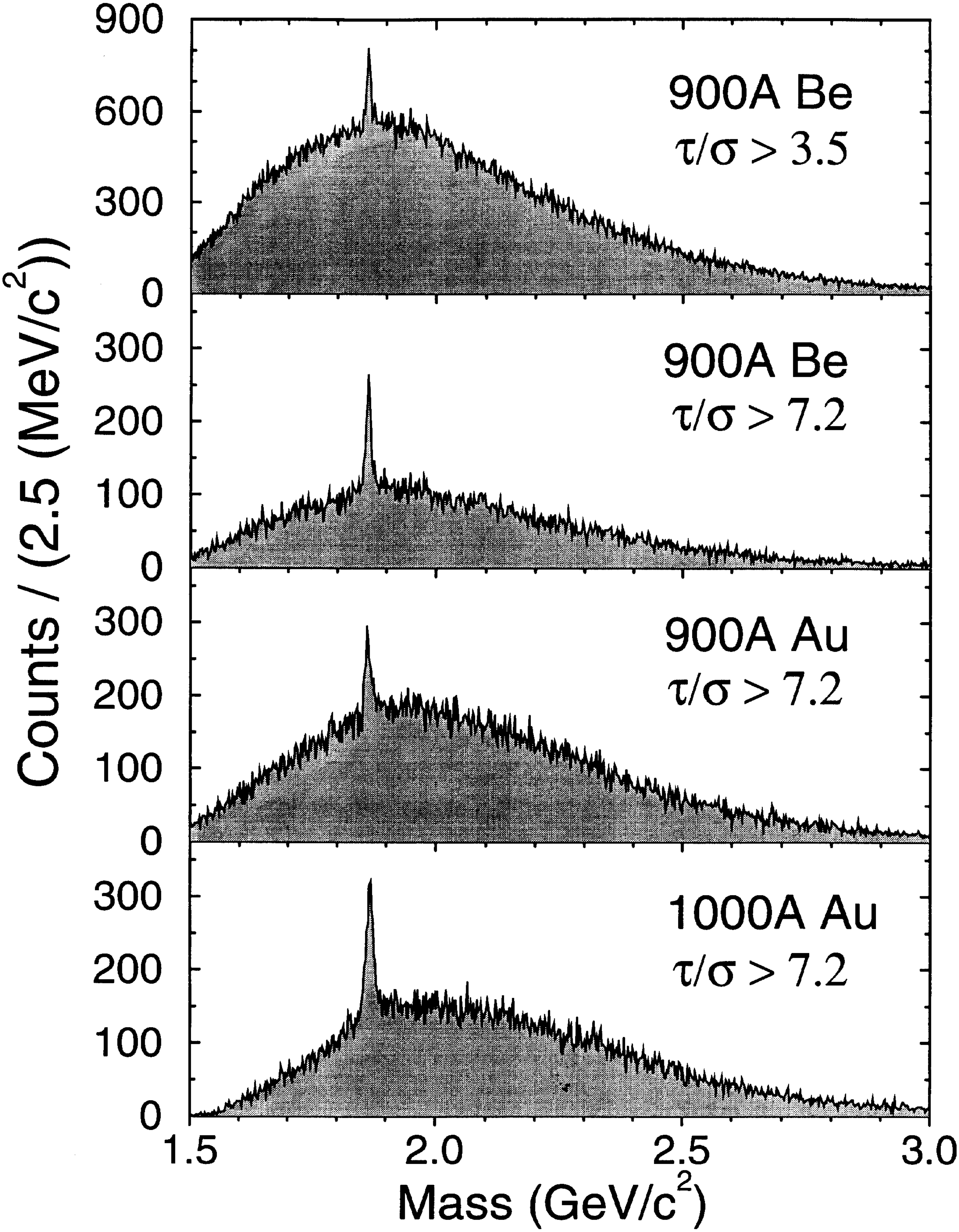
900
600
300
0
300
200
100
0
300
200
100
0
300
200
100
0
900A Be
τ/σ > 3.5
900A Be
τ/σ > 7.2
900A Au
τ/σ > 7.2
1000A Au
τ/σ > 7.2
Counts / (2.5 (MeV/c²))
1.5
2.0
2.5
3.0
Mass (GeV/c²)

Figure 1

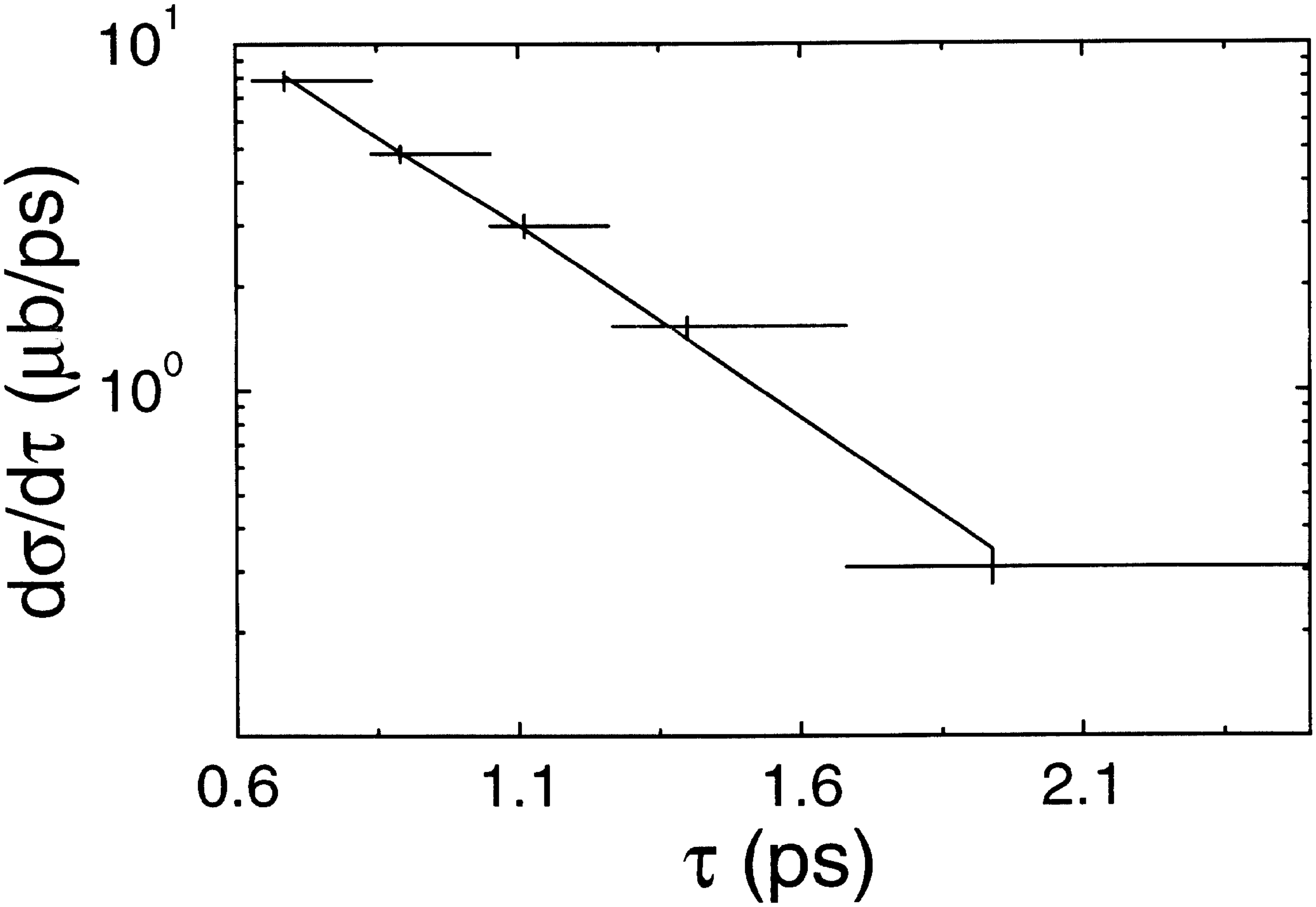

Figure 2

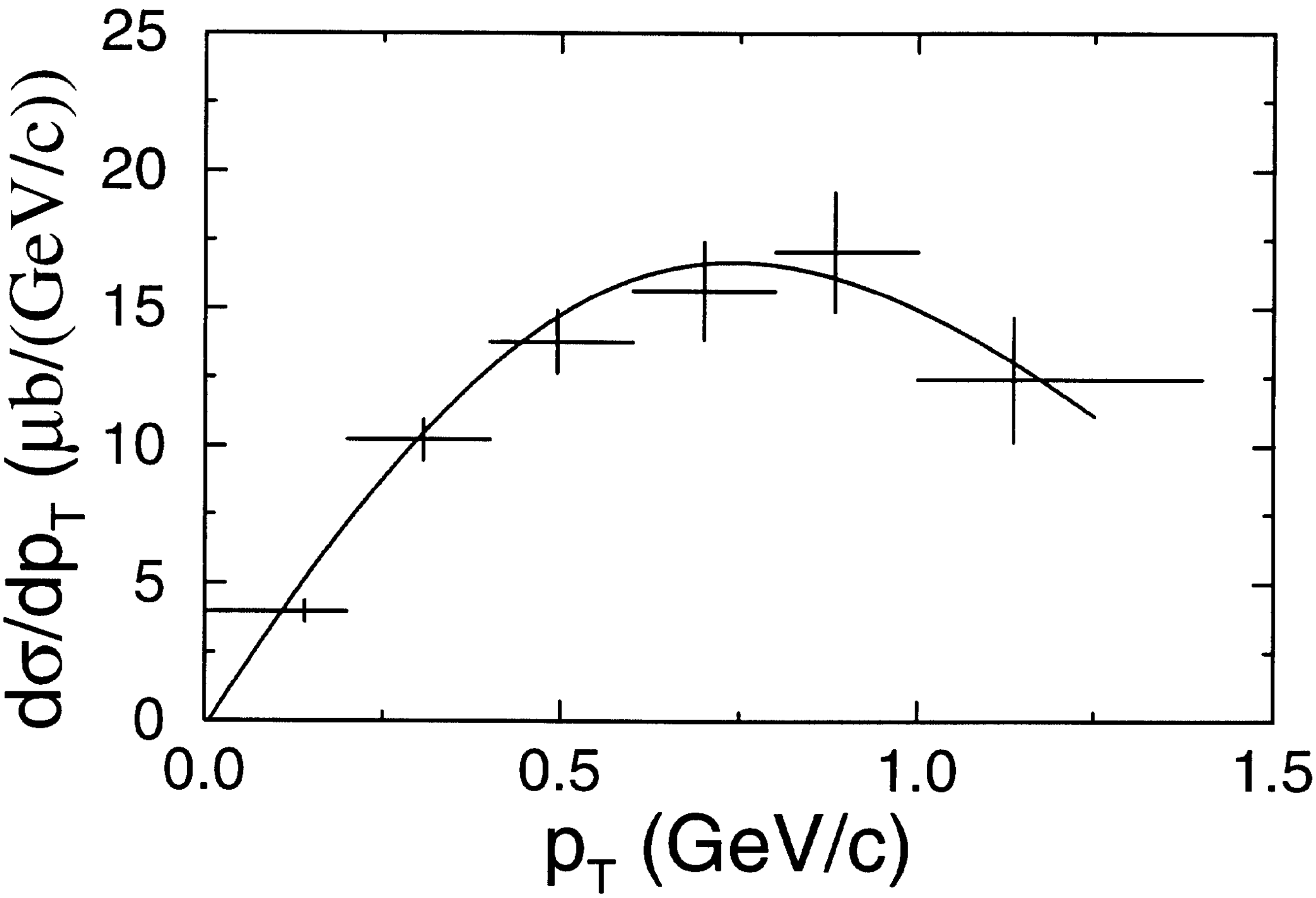

Figure 3